

# Bloch electron in a magnetic field: Mixed dimensionality and the magnetic-field- induced generalized quantum Hall effect

by Mark Ya. Azbel

**The energy spectrum of a Bloch electron in a magnetic field is one-dimensional. This leads to the Peierls instability and the magnetic-field-induced transition to the quantized Hall effect. The wave function is two-dimensional. This decreases the Peierls gap and makes it exponentially vanishing with magnetic field. Disorder lifts the degeneracy and one-dimensionality of the spectrum. High disorder yields a metallic behavior. Intermediate disorder**

**leads to the generalized quantized Hall effect. The latter has a finite magnetoresistance as a semimetal, and Hall plateaus similar to the quantized ones, but they may have any value of the effective charge.**

## 1. Experiment

Experiments [1] in quasi-two-dimensional (2D) Bechgaard salts  $(\text{TMTSF})_2\text{X}$ ,  $\text{X} = \text{ClO}_4, \text{PF}_6, \text{ReO}_4$ , have clearly demonstrated Hall resistance plateaus similar to but different from those in the quantized Hall effect (QHE).

In Table 1  $\rho_{xy}$  and  $\rho_{xx}$  are, respectively, the Hall resistivity and magnetoresistivity (per crystallographic  $z$ -plane);  $c$  is the (smallest) bandwidth along the magnetic field  $H$ ;  $\epsilon_F$  is the Fermi energy;  $m^*$  is the effective mass;  $n$  is the charge density in the  $xy$  plane;  $j$  is the filling factor;  $j_{\text{eff}}$  is the effective filling factor;  $\vec{H} \parallel z$ . Three features of the Bechgaard salts sound strange for QHE:

©Copyright 1988 by International Business Machines Corporation. Copying in printed form for private use is permitted without payment of royalty provided that (1) each reproduction is done without alteration and (2) the *Journal* reference and IBM copyright notice are included on the first page. The title and abstract, but no other portions, of this paper may be copied or distributed royalty free without further permission by computer-based and other information-service systems. Permission to *republish* any other portion of this paper must be obtained from the Editor.

1.  $j_{\text{eff}}$  is orders of magnitude less than  $j$ .
2. The effective charge  $\nu$  is neither an integer nor an odd-denominator fraction.
3. A very high  $n \approx 2 \times 10^{14} \text{ cm}^{-2}$  implies  $k_F t \approx 2000$ ,  $k_F r_c > 100$  ( $k_F$  is the Fermi wave vector,  $r_c = \hbar k_F c / eH$ ;  $t$  is the mean free path), and thus rules out any localization [2], which is so crucial for QHE.

Gor'kov and Lebed' [3] were the first to understand that quasi-1D materials undergo a magnetic-field-induced transition (MFIT). Although this transition is related to the Peierls instability [4], the gap, which opens at the Fermi energy, leads to a QHE rather than to an insulator. Indeed, a completely filled sub-band is in fact [5] a broadened Landau level which carries electrons or holes, whereas a "conventional" Peierls transition yields a "true" band with electron and hole currents compensating each other. Defects [5] lead to a generalized QHE (GQHE) with an "irregular" effective charge, in agreement with experiments [6].

In this paper I demonstrate that the physics of the GQHE is related to the "dimensionality mixture" for a 2D Bloch electron in a magnetic field. Its highly degenerate spectrum is quasi-1D, whereas its wave function is 2D. I study the resulting unusual Peierls transition, where defects lift the spectrum degeneracy, make it quasi-2D, and lead to the effective charge  $\nu$ . The GQHE emerges at intermediate randomness. It is flanked by the QHE on the "very pure sample side" and by a metallic phase on the "dirty sample side." A complete phase diagram, METAL-QHE-GQHE, is presented.

In Section 2, I discuss the Peierls instability in the presence of randomness for  $H = 0$  and  $H \neq 0$ . Section 3 considers the implications of the "1D" spectrum for the magnetic field-induced transition (MFIT). The GQHE is discussed in Section 4, and Section 5 deals with the METAL-QHE-GQHE phase diagram.

## 2. The Peierls instability

Consider the Peierls instability in magnetic field  $\hat{H} \parallel z$ . In the plane  $xy$ , the dispersion relation in the Bechgaard salts is

$$\epsilon = \frac{\hbar^2 k_x^2}{2m^*} + a \cos(k_y b), \quad (1)$$

where  $\epsilon_F \approx 1500 \text{ K}$ ,  $a \approx 300 \text{ K}$ ,  $m^* \approx 10^{-27} \text{ g}$ ,  $b \approx 7 \text{ \AA}$ . The Peierls substitution [7],

$$\hat{k} \rightarrow \frac{1}{i} \nabla - \frac{e}{\hbar c} \hat{A},$$

in the vector potential Landau gauge,  $A = A_y = -Hx$ , yields the Schrödinger equation for the wave function  $\psi$ :

$$-\frac{\hbar^2}{2m^*} \frac{\partial^2 \psi}{\partial x^2} + a \cos\left(\frac{b}{i} \frac{\partial}{\partial y} + \frac{eHb}{\hbar c} x\right) \psi = \epsilon \psi. \quad (2)$$

Choosing  $\psi = \chi \exp(ik_y y)$ , one finds

**Table 1** Experimental conditions and results.

"Common" QHE	Bechgaard salts
<i>Conditions</i>	
Two-dimensional	Quasi-two-dimensional ( $c/\epsilon_F < 0.003$ )
$\frac{\hbar eH}{m^*c} >   \text{Potential}  $	$\frac{\hbar eH}{m^*c} \ll   \text{Potential}  $
No periodic potential	Strong periodic potential along $y$
$j \equiv nch/eH \approx 1$	$100 \leq j \leq 250$
<i>Results</i>	
$\rho_{xy} = \frac{h}{e^2 j}$	$\rho_{xy} = \frac{h}{e^2 j_{\text{eff}} \nu}$ , $j_{\text{eff}} \ll j$ , $\nu \approx 1$
$\rho_{xx} = 0$	$\rho_{xx} \neq 0$
Electrons or holes	Electron $\Leftrightarrow$ hole transitions

$$\chi'' + \frac{2m^*}{\hbar^2} \left[ \epsilon - a \cos \frac{eHb}{\hbar c} (x - x_0) \right] \chi = 0, \quad (3)$$

$$x_0 = -\frac{\hbar k_y}{eH}. \quad (4)$$

This is the Mathieu equation. Its gaps are  $\propto \exp(-2000/H_T)$ , where  $H_T$  is the magnetic field in teslas. Clearly, they are absolutely negligible. However, Equation (3) in  $x_1 = x - x_0$  is effectively the Schrödinger equation in a 1D periodic potential. Thus, it is unstable [3] with respect to the Peierls gap formation [4]. The perturbative SDW potential  $V_0 \cos(2k_F x)$  generates a gap  $\Delta$  at  $\epsilon = \epsilon_F$  and decreases the electron energy by  $\approx \Delta^2 \ln(\epsilon_F/\Delta)$ . For sufficiently small  $\Delta$ , this is always beneficial, since the SDW energy increase is  $\propto \Delta^2$ . The gap formation is clearly related to the 1D nature of the spectrum, i.e., to the degeneracy of the spectrum with respect to  $k_y$ . The wave function remains [8] 2D. To make the impact of this "dimensionality difference" explicit, consider the Peierls gap formation in more detail in a "conventional" 1D case (when  $H = 0$ ) and in the Equation (3) situation. When defects are present, this analysis turns out to be of importance.

## 3. 1D Schrödinger equation

Consider the 1D Schrödinger equation with a periodic potential  $u(x)$ :

$$\psi'' + \frac{2m^*}{\hbar^2} (\epsilon - u) \psi = 0. \quad (5)$$

When  $\epsilon > \max u$ , the exact solution to Equation (5) in the allowed band may be presented in the form

$$\psi_{\pm} = k^{-1/2} \exp\left(\pm i \int k dx\right), \quad (6)$$

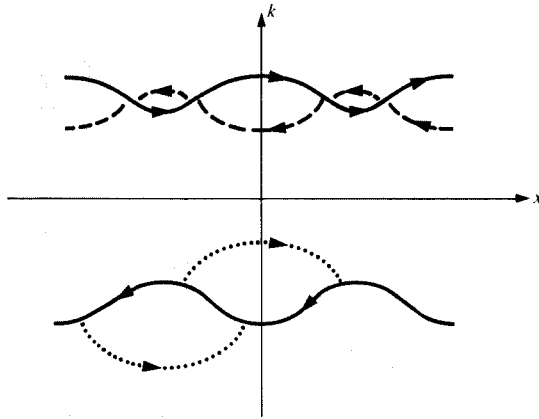


**Figure 1**

One-dimensional nesting in a magnetic field. Dashed lines—closed orbits with clockwise and anticlockwise motion. Dotted lines—“best nesting” in Equation (3); largest closed-orbit areas with clockwise electron and anticlockwise hole motion.

where  $k(x)$  is determined by the equation

$$k^2 = \frac{2m^*}{\hbar^2} (e - u) + \frac{3k'^2 - 2kk''}{4k^2}. \quad (7)$$

In the quasi-classical limit,  $k^2 \approx 2m^* (e - u)/\hbar^2$ —see **Figure 1**.

A perturbative potential  $V$  nests the two branches, generating a gap

$$\Delta = \int \psi_+ V \bar{\psi}_- dx. \quad (8)$$

By Equation (8), the largest gap is provided by

$$V = V_0 \text{Re}(\psi_+ \bar{\psi}_-). \quad (9)$$

Then

$$\Delta = V_0 \int |\psi_+ \bar{\psi}_-|^2 dx \approx V_0. \quad (10)$$

Defects lead to a random contribution to  $u$  in Equation (5) (and to localization). Still, the choice(s) of the perturbative potential may allow for the gap  $\Delta \approx V_0$  in the spectrum.

The picture for Equation (3) is drastically different, since  $\chi = \chi(x - x_0)$  depends on the orbit center coordinate  $x_0$ . One *cannot* choose the same “good for all  $x_0$ ” factor  $V$  of Equation (9). The “2D nature” of the wave function results in a gap, which is *much smaller* than  $V_0$  and which  $\rightarrow 0$  when  $H \rightarrow 0$ . The “best” nesting in Equation (3) (leading to the largest gap) is related to the largest closed-orbit areas (dotted lines in Figure 1), which may correspond to clockwise electrons or anticlockwise holes. [For the best nesting in Equation (2), see [9]]. The quantization of

magnetic flux through closed orbits leads to the Landau levels. Magnetic breakdown tunneling between the orbits broadens the levels into Landau sub-bands separated by narrow gaps. If the Fermi energy is in the largest gap, then the corresponding filling factor is

$$j_{\text{eff}} \approx \frac{1}{2\pi} (\text{dotted area}) \propto H^{-1}. \quad (11)$$

In the quasi-classical limit, electron and hole orbits are almost degenerate; hence easy electron-hole and hole-electron transitions occur.

The largest gap is [5, 9]

$$\Delta \propto V_0 H^{-1/3}. \quad (12)$$

Given the relation between  $\Delta$  and  $V_0$ , thermodynamics determines  $V_0$ . The minimum of the combined electronic [ $\propto \Delta^2 \ln(\epsilon_F/\Delta)$ ] and SDW ( $\propto \Delta^2$ ) energies yields [5, 9]

$$\ln V_0^{-1} \propto j_{\text{eff}}^{-2/3}. \quad (13)$$

The random potential  $W$  contribution to Equations (2) and (3) lifts the spectrum degeneracy. Hence, it may be impossible to generate the gap for all  $x_0$ 's at the same energy. Even the best nesting may leave a small density of states at the Fermi energy. Physically this is most explicit in the quasi-classical limit ( $k_F r_c \gg 1$ ) when  $|\nabla W| \ll (v/c)eH$ , where  $\tilde{v} = 1/\hbar \partial \epsilon / \partial \vec{k}$  is the velocity. Then, in the leading approximation we find the Lorentz equation  $\hbar \dot{\vec{k}} = (e/c) \vec{r} \times \vec{H}$  and

$$\vec{r} = \vec{r}_0 + \frac{\hbar c \vec{H}}{e H^2} \times (\vec{k} - \vec{k}_0). \quad (14)$$

Now the conservation of the total energy  $\epsilon_i$  implies, by Equation (14),

$$\epsilon_i = \epsilon(\vec{k}) + W(\vec{r}) = \epsilon(\vec{k}) + W \left[ \vec{r}_0 + \frac{\hbar c \vec{H}}{e H^2} \times (\vec{k} - \vec{k}_0) \right]. \quad (15)$$

Thus, the kinetic energy

$$\epsilon(\vec{k}) = \epsilon_i - W \left[ \vec{r}_0 + \frac{\hbar c \vec{H}}{e H^2} \times (\vec{k} - \vec{k}_0) \right] \quad (16)$$

changes with  $k$  and depends on the initial  $\vec{r}_0$  and  $\vec{k}_0$ . (Note that when  $W = 0$ ,  $\epsilon$  is conserved.) The corresponding smearing of the gap may be much larger than the conventional broadening  $\hbar/\tau = \hbar v/\ell$ , where  $\tau$  is the mean free path time. For instance, if one considers an “average” variation  $W$  over distances of order  $\ell$ , then the characteristic gap smearing is

$$\delta W \approx (W/\ell) r_c \equiv \frac{W}{\Omega \tau} = \frac{\hbar}{\tau} \frac{W}{\hbar \Omega} \gg \hbar/\tau,$$

since  $W \gg \hbar \Omega = (\hbar e H / m^* c)$ —see Table 1. If  $\delta W > \Delta$ , then any nesting yields states at  $\epsilon_F$  (although their density may be low). They lead to finite dissipation and magnetoresistivity.

#### 4. QQHE theory

The theory of the QQHE may be constructed by introducing into Figure 1 the probability  $p$  of a magnetic breakdown and the probability matrix  $\hat{\tau}$  of random intra- and inter-branch scattering per unit time. The average distance traveled along  $x$  is  $\approx r_c/q$ , where  $q \equiv 1 - p$ . If  $r_c/q \ll l$ , then the orbit is effectively closed, and one may expect a "conventional" QHE. This, in particular, happens when  $l \rightarrow \infty$ . If  $r_c/q \gg l$ , then scattering occurs before an electron "learns" that its orbit is closed, and it may "presume" it to be effectively open. This happens, in particular, when  $q = 0$  (truly open orbit). To understand the physics of the general situation, consider first the latter case. Suppose the electric field  $E$  is along the  $\xi$  direction, and let  $\eta$  be a coordinate perpendicular to  $\xi$  (the crystallographic axes are  $x$  and  $y$ ). Then the Lorentz equation

$$\hbar \dot{\vec{k}} = \left( \frac{e}{c} \hat{\tau} \times \vec{H} \right) + e\vec{E} \quad (17)$$

implies that

$$\xi = \xi_0 - \hbar c(k_y - k_0)/eH. \quad (18)$$

The total energy  $\epsilon_i$  conservation

$$\epsilon_i = \epsilon(\vec{k}) - eE\xi \quad (19)$$

yields

$$\epsilon(\vec{k}) = \epsilon_i - e(\xi_0 + \hbar ck_0/eH)E + \hbar ck_\eta E/H. \quad (20)$$

[Note that, in contrast to Equation (16), Equation (20) is an exact formula.] The energy  $\epsilon(\vec{k})$  slowly decreases until, close to the self-crossing (at  $H = 0$ ) energy  $\epsilon_{\min}^{\text{sc}}$ , an orbit has a reflection point. The corresponding change in the energy is large, so one must consider a "complete" Bloch dispersion, e.g.,

$$\epsilon = \cos(k_x b_x) + a \cos(k_y b) \quad a < 1. \quad (21)$$

After the reflection,  $k_y$  decreases, and the increase in the energy, by Equation (20), ultimately also leads to the reflection in the vicinity of the hole self-crossing energy  $\epsilon_{\max}^{\text{sc}}$ , and so on—see Figure 2. By Equation (19),

$$\Delta\xi = \frac{\Delta\epsilon}{eE} \quad \Delta\epsilon = \epsilon_{\max}^{\text{sc}} - \epsilon_{\min}^{\text{sc}}; \quad (22)$$

i.e.,  $\Delta\xi$  is finite, but usually *very large*, and  $E > \Delta\epsilon/eL$  leads to nonlinearity ( $L$  is the sample size along  $\xi$ ). By Equation (17), the average velocity  $\langle \dot{\eta} \rangle$  along  $\eta$  is

$$\langle \dot{\eta} \rangle = -\frac{cE}{H} + \frac{c\hbar}{eH} \lim_{\Delta t \rightarrow \infty} \frac{\Delta k_\xi}{\Delta t}, \quad (23)$$

where  $\Delta k_\xi \neq 0$ . Equation (23) gives a renormalized "conventional" Hall velocity ( $-cE/H$ ). (A closed orbit is periodic, and its  $\Delta k_\xi = 0$ .) To calculate  $\langle \dot{\eta} \rangle$ , complement Equation (20) with the Hamilton equation

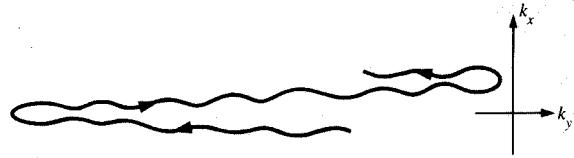


Figure 2

Open orbit (in  $\vec{k}$ -space) in crossed electric and magnetic fields.

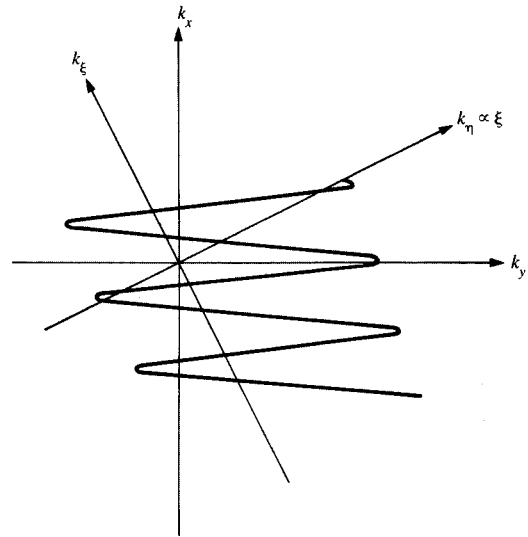


Figure 3

Orbit center motion.

$$\dot{\vec{r}} = \frac{1}{\hbar} \frac{\partial \epsilon}{\partial \vec{k}},$$

which with Equation (18) relates  $k_\xi$  in Equation (17) to  $k_\eta$ :

$$\frac{1}{\hbar} \frac{\partial \epsilon}{\partial k_\xi} = \dot{\xi} = -\hbar ck_\eta/eH. \quad (24)$$

Equations (20) and (24) allow one to calculate  $k_y(t)$  and  $k_\xi(t)$ . Then Equation (23) determines  $\langle \dot{\eta} \rangle$ ,

$$\langle \dot{\eta} \rangle = \frac{\nu cE}{H} \quad \nu = 1 - \frac{2\pi |k_x^{\min}|}{b \int_0^{2\pi/b} |k_x| dk_y}. \quad (25)$$

The orbit is extended along  $\eta$ , but  $\langle \dot{\eta} \rangle \propto E$  is usually very small. See Figure 3 for the orbit center motion.

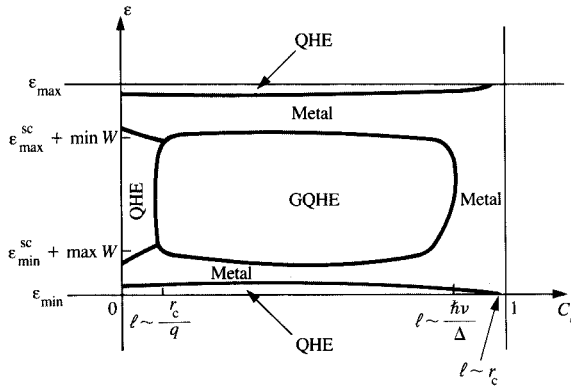


**Figure 4**

METAL-QHE-GQHE phase diagram.

Now consider a general case with finite  $l$  and  $q$ . In the quasi-classical limit, we have

$$1 - q = p \propto \exp\left(-\int |k_x| dx\right). \quad (26)$$

Calculating the integral in the classically forbidden region [generated by the gap  $\Delta$  from Equation (12)], one arrives at

$$\ln p^{-1} \approx j_{\text{eff}}^{4/3} V_0^2. \quad (27)$$

Now, solving the master equation, one determines the Hall resistivity per plane [5]:

$$\rho_{xy} = \frac{\hbar}{e^2 \nu j_{\text{eff}}}, \quad (28)$$

where  $j_{\text{eff}}$  is an integer and  $\nu$  is the effective charge. In a general case [5],

$$\nu = 1 - \frac{2\pi}{bS} \frac{|k_x^{\text{min}}| + \frac{1-q}{q} \int_0^T \hat{\tau}_*^{-1} |k_x| dt}{1 + \frac{1-q}{q} \int_0^T \hat{\tau}_*^{-1} dt}. \quad (29)$$

Here

$$S = \int_0^{2\pi b} |k_x| dk_y,$$

is the orbit area,  $T$  is the period:

$$T = \frac{c}{eH} \frac{\partial S}{\partial \epsilon},$$

and the subscript \* denotes the interbranch scattering.

Clearly,  $\nu$  may take any value and can be of either sign in the GQHE.

## 5. METAL-QHE-GQHE phase diagram

When a sample is sufficiently dirty,  $\hbar v/l > \Delta$ , there is no gap nor a MFIT. When a sample is very clean,  $l > r_c/q$ , the orbits are closed,  $k_x^{\text{min}} = 0$  in Equation (29), and  $\nu = 1$ ; i.e., one observes MFI QHE.

Until now I have discussed only orbits which are open at  $H = 0$ . If the Fermi energy corresponds to a closed (at  $H = 0$ ) orbit, then the Landau sub-band is exponentially narrow,  $\propto \exp(-k_F r_c)$ , and it makes “exponentially little sense” to open a gap in it. Since  $k_F r_c \gg 1$  implies no localization [2], the phase is metallic, with a conventional Hall effect. Localization, together with QHE, develops near the band edges, where  $k_F r_c \lesssim 1$ . (Note that throughout the paper I assume a 2D situation.)

According to Equation (16), when

$$(W_{\text{max}} - W_{\text{min}}) < (\epsilon_{\text{max}}^{\text{sc}} - \epsilon_{\text{min}}^{\text{sc}}),$$

there are two boundaries between open and closed orbits, at

$$\epsilon = \epsilon_{\text{max}}^{\text{sc}} + W_{\text{min}}$$

and at

$$\epsilon = \epsilon_{\text{min}}^{\text{sc}} + W_{\text{max}}.$$

Thus, at  $T = 0$  the 2D phase diagram in the energy  $\epsilon$ -impurity concentration ( $C_i$ ) plane appears as in **Figure 4**.

The following are some remarks concerning the diagram:

1. The boundaries between the GQHE and the QHE are obviously smeared.
2. The boundaries between the GQHE and metallic phases have in fact a complicated shape, since the Landau spectrum is complicated in the vicinity of self-crossing orbits [10].
3. There are two “quasi-mobility edges” at METAL-QHE boundaries. These are not “true” mobility edges, since an unrealistically large  $L \gg l \exp(2\pi/lb)$  implies localization at all energies.

## References and note

1. For a review and references, see L. P. Gor'kov, *Sov. Phys. Rep.* **27**, 809 (1984) and *Proceedings of Yamada Conference XV on Quasi-1-D Conductors, Physica* **B143** (1986).
2. When  $H = 0$ , the 2D localization length  $\xi$  is of the order  $\exp(k_F l) \approx 10^{1000}$ . When  $H \neq 0$ , one may assume the scaling  $\ln \xi \approx k_F l F(r_c/l)$ , with  $\xi$  being finite and independent of  $l$  when  $l \rightarrow \infty$ . Then  $r_c \ll l$  yields  $\xi \propto \exp(k_F r_c) > 10^{40}$ . Note that in the latter case adjacent orbit centers are separated by distances which are small compared to the orbit size  $r_c$  and allow for easy inter-orbit tunneling and “delocalization,” if the random potential changes little at  $r_c$ .
3. L. P. Gor'kov and A. G. Lebed', *J. Phys. (Paris) Lett.* **45**, L433 (1984).
4. R. E. Peierls, *Quantum Theory of Solids*, Chapter 5, Clarendon Press, Oxford, 1964.
5. M. Ya. Azbel, Per Bak, and P. M. Chaikin, *Phys. Rev. Lett.* **59**, 926 (1987); *Phys. Rev. A* **34**, 1392 (1986).
6. P. M. Chaikin, Mu-Yong Choi, J. F. Kwak, J. S. Brooks, K. P. Martin, M. J. Naughton, E. M. Engler, and R. L. Greene, *Phys. Rev. Lett.* **51**, 2333 (1983); M. Ribault, D. Jerome, J. Tuchendler, C. Weyl, and K. Bechgaard, *J. Phys. Lett.* **44**, 1953 (1985).

7. R. E. Peierls, *Z. Phys.* **80**, 763; *ibid.* **81**, 186 (1933).
8. However, see M. Ya. Azbel, submitted to *Phys. Rev. Lett.*
9. D. Poilblanc, G. Montaubaux, M. Heritier, and P. Lederer, *Phys. Rev. Lett.* **58**, 270 (1987).
10. See, e.g., M. Ya. Azbel, *Zh. Eksp. Ter. Fiz.* **39**, 1276 (1960) and references therein.

*Received September 9, 1987; accepted for publication  
October 19, 1987*

**Mark Ya. Azbel** *Department of Physics, Tel-Aviv University, Tel-Aviv, Israel.* Professor Azbel received an M.A. (1953) and a Ph.D. (1955) from Kharkov University, Kharkov, USSR, and the D.S.C. (1957) from the Institute of Physical Problems, Moscow, USSR, for his prediction (with E. Kaner) of cyclotron resonance in metals (with L. Landau and P. Kapitza on the committee). From 1957 to 1964 he was a full professor at Kharkov University and the Kharkov Physical-Technical Institute. In 1964, he was appointed a full professor at Moscow State University and Department Director at the Landau Institute for Theoretical Physics—positions he held until 1972. Professor Azbel applied for an exit visa in 1972 and in 1977 was allowed to leave the Soviet Union. Since 1977 he has been a full professor at Tel-Aviv University, and is currently an adjunct professor at the University of Pennsylvania, Philadelphia. He has published more than 200 papers in scientific journals, and about 100 articles in literary journals. Professor Azbel is an APS Fellow; he has received two Lomonsov Prizes from Moscow University, two nominations for the Lenin Prize, and two nominations for the Soviet Academy of Science.